

Volatility Based Change Detection in Data Streams

Alireza Ahrabian, Nazli Farajidavar, Clive Cheong-Took and Payam Barnaghi

Abstract— This work develops a class of techniques for the sequential detection of transient changes in the variance of time series data. In particular, we introduce a class of change detection algorithms based on the windowed volatility filter. The first method detects changes by employing a convex combination of two such filters with differing window sizes, such that the adaptively updated convex weight parameter is then used as an indicator for the detection of instantaneous power changes. Furthermore, a multi-sensor extension of the algorithm is also proposed, that exploits cooperation between sensors so as to enable a more accurate update of the convex weight parameter. The second method provides an estimate of the change point location, using a statistical significance test along with a new change point estimator, based on the differenced output of the volatility filter. Finally, the performance of the proposed algorithms were evaluated on both synthetic and real world data.

Index Terms— Volatility Change Detection, Transient Detection.

I. INTRODUCTION

The piecewise segmentation of time series data into intervals with similar stochastic characteristics is often important in the exploratory analysis of data and is generally referred to as change detection. With rapid growth and advancements in the Internet of Things (IoT) and sensing technologies [1] [2], there is a need for effective and adaptive methods to identify and analyse activities in time series data [3] [4]. In particular the partitioning of data into segments of constant volatility (variance/standard deviation) has particularly interesting applications for fields ranging from the segmentation of biomedical data [5] to audio segmentation [6] [7].

Algorithms proposed for estimating the transition times for data points with transient changes in the variance are generally divided into two categories: i) Offline algorithms that use the entire data set so as to estimate the location of the change points and ii) online (sequential) methods, where data is only available up to the current time sample being analysed. Early research primarily focused on developing statistical significance based change detection algorithms [8], where in particular the work in [8] proposed a method based on the cumulative sum of squares in combination with a statistical significance test so as to provide an estimate of change points. More recently, algorithms based on maximum likelihood have been proposed [9] [10], where an optimal segmentation method based on the maximum a posteriori estimate was developed [10]. However, owing to the combinatorial nature of the problem, numerical optimisation techniques such as simulated annealing are required in order to identify solutions that

converge to the approximate global maximum or minimum within a reasonable time frame. In order to overcome the computational complexity of the numerical optimisation based algorithms, techniques based on Monte Carlo Markov Chain (MCMC) methods are employed in [9] and [11] to further reduce the computational cost of calculating the transition time points.

Many real world practical change detection problems require sequential algorithms which are not only capable of detecting with the smallest possible delay the change in the volatility of the data sequence (event detection), but also potentially providing a good estimate of the change point location (online data segmentation). The work in [12] introduced a method based on the likelihood ratio test that includes a simple threshold and test statistic for both detecting and estimating the location of the change in the volatility of the time series data. Furthermore, the work in [9] proposed a threshold independent sequential change detection method using the minimum description length (MDL), while an on-line kernel-Support Vector Machine (k-SVM) based change detection method with high accuracy was proposed in [6]. However, such methods often have drawbacks, that include the following: high computational complexity, low accuracy of change point location estimate and high detection latency.

We introduce a class of change detection algorithms based on windowed volatility filters [13]. The first proposed algorithm seeks to detect such transient power/volatility variations as rapidly as possible, this is achieved by employing a convex combination of two such filters, where a state change is detected by selecting the appropriate filter given the statistics of the data points. The rationale behind the proposed method arises from the trade off that exists between steady state accuracy and convergence speed of volatility filters. By using a collaborative adaptive filter [14] [15], the proposed method seeks to overcome this trade off by updating the weights of the respective windowed volatility filters, thereby providing an indicator for detecting variations in the power of the time series data. Furthermore, a multi-sensor extension of the algorithm based on a cooperative adaptive filtering algorithm [16] is also developed. The second algorithm provides an estimate for the change point location. This is achieved by making use of a new estimator based on the differenced output of the volatility filter, for both detection and change location estimation. The performance of the proposed change detection algorithms are verified on both synthetic and real world data sets.

The organisation of this paper is as follows: Section 2 outlines the change point problem statement and provides an overview of different sequential change detection methods. Section 3 presents the class of proposed change point algorithms based on volatility filtering and Section 4 assesses the performance of the algorithm through simulations. Section 5

The authors Alireza Ahrabian, Nazli Farajidavar and Payam Barnaghi are with the Department of Electrical and Electronic Engineering, Institute for Communication Systems at the University of Surrey, GU2 7HX, U.K. (email: {a.ahrabian, n.farajidavar, p.barnaghi}@surrey.ac.uk).

Clive Cheong-Took is with the Department of Computer Science at the University of Surrey GU2 7HX, U.K. (email:c.cheongtook@surrey.ac.uk)

provides a conclusion and briefly discusses the future work.

II. BACKGROUND AND PROBLEM OUTLINE

Given a sequence of data points $\{x(1), x(2), x(3), \dots, x(t)\}$ drawn from a zero mean Gaussian distribution with piecewise constant variance; there exists an unknown sequence of transition time instances $\{\tau_1, \tau_2, \dots, \tau_t\}$ at which a change in the variance of the Gaussian distribution where the data points are drawn from occurs (an example of such a time series is shown in Fig. 1). Accordingly, this work seeks to address the problem of developing two categories for change detection: 1) the first category seeks to detect a transition/change in the power of time series data with the shortest possible latency (where this is particularly useful for event/anomaly detection); 2) the second category algorithm seeks to both detect a change in the power, as well as providing an accurate estimate of the location of the transition times $\{\hat{\tau}_1, \hat{\tau}_2, \dots, \hat{\tau}_t\}$, thus enabling for higher performance sequential time series segmentation (this is particularly useful for the exploratory data analysis of events).

We now provide an overview of sequential/online volatility based change detection algorithms, namely the generalised likelihood ratio based method proposed in [12], the minimum description length (MDL) likelihood ratio technique [9] and the kernel-SVM state change detector in [6].

The generalised likelihood ratio (GLR) change detector algorithm proposed in [12] seeks to both detect changes in the time series volatility as well as providing estimates of the change locations. The problem is formulated as follows:

$$\begin{aligned} H_0 : \sigma &= \sigma_0 \quad \text{for } 1 \leq k \leq n \\ H_1 : \sigma &= \sigma_1 \quad \text{for } 1 \leq k \leq r \\ &\text{and } \sigma = \sigma_2 \quad \text{for } r < k \leq n \end{aligned} \quad (1)$$

where the ratio of the likelihood functions (assuming Gaussian distribution) of the respective hypotheses were determined and thresholds of the likelihood ratio were utilised for both change detection and location estimation.

The sequential minimum description length (MDL) is a threshold-independent change detection algorithm which utilises the likelihood ratio. That is for a segment of data the likelihood ratio (the same hypothesis as outlined above) is initially maximised so as to first obtain an estimate of a potential change point location. Next the significance of the estimated change point location is evaluated using the minimum description length criterion. The method then seeks to determine the number of partitions $\hat{l} \in [1, 2]$ by maximising a penalised cost function [9], $MDL(l|y)$:

$$\hat{l} = \underset{\hat{l} \in [1, 2]}{\operatorname{argmax}} MDL(l|y) \quad (2)$$

The $MDL(l|y)$ is dependent on the likelihood estimate of the data segment, where $\hat{l} = 1$ indicates the existence of one change point within the analysed data segment and $\hat{l} = 2$ indicates the absence of any. Finally, in [6], the authors proposed the KCD, an online kernel change detection algorithm where kernel descriptors have been used to represent the immediate

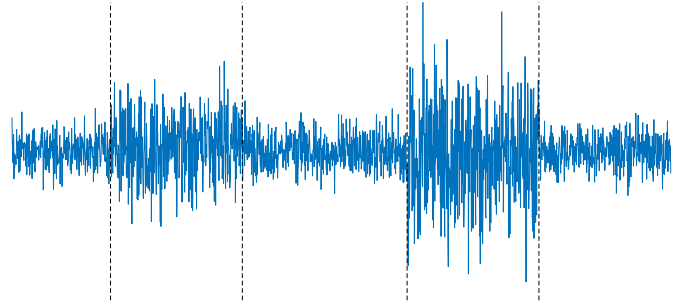


Fig. 1. Time series data with instantaneous power changes, where the vertical dashed lines show the location of the transition points.

past and future set time segments and a similarity measure based on single class Support Vector Machines (SVM) is proposed for change point estimation.

III. PROPOSED ALGORITHMS

This work proposes two computationally inexpensive online change detection algorithm based on volatility filtering given the data sequence, $\{x(1), x(2), x(3), \dots, x(t)\}$, the output of the volatility filter, $\sigma_x(t)$, is defined as the moving windowed standard deviation of the past T data points, that is

$$\sigma_x^2(t) = \frac{1}{T} \sum_{i=0}^{T-1} x^2(t-i) - \hat{\mu}^2 \quad (3)$$

where $\hat{\mu}$ corresponds to the sample mean of the past T data points. The first algorithm combines both adaptive and volatility filters so as to only detect changes in the power of time series data as rapidly as possible, while the second proposed algorithm maps the output of the volatility filter in order to develop an estimator for the change point location.

A. Adaptive Filtering Based Change Detection Method

The first proposed method seeks to develop a change detection algorithm through the use of a collaborative adaptive filters [17] [14] [15]. This is achieved by tracking changes in the instantaneous power using a convex combination of two volatility filters of differing window sizes. Where a volatility filter with a small window size is able to track transient changes in the time series power. However, in the steady state the estimate of the change in the power of the signal is not accurate; while a volatility filter with a large window size has stable steady state estimates of volatility. By adaptively estimating the convex weight parameter, such that if a significant transient change has occurred then volatility filter with a small window size provides a more optimal (least squared sense) solution than the volatility filter with the large window size. As a result, by tracking the estimate of the convex weight combiner, it can be determined whether or not a change has occurred. Furthermore, we extend the proposed method for data sets drawn from multiple sensors, by using an adaptive filtering architecture that utilises cooperative strategies [16] to enhance both convergence and steady state accuracy of the convex weight parameter. Given a signal

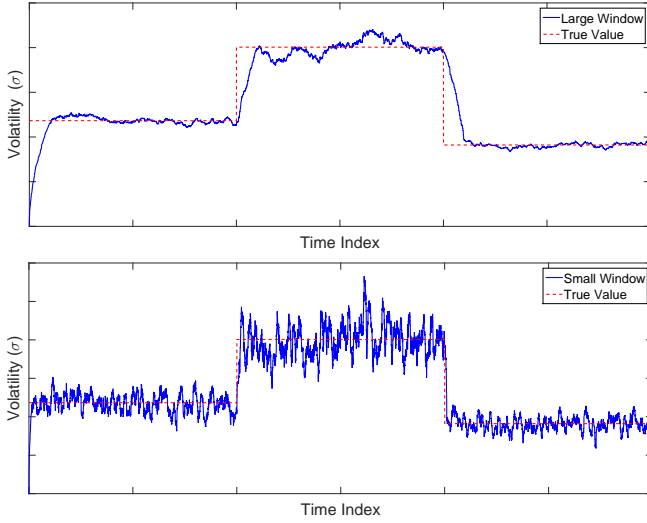


Fig. 2. Figure showing the estimated volatility for time series with instantaneous power changes. (Upper panel) Shows the output of the ‘slow’ and (lower panel) the output of the ‘fast’ volatility filter.

$x(t)$, consider the following

$$\sigma_f^2(t) = \frac{1}{T_f} \sum_{i=0}^{T_f-1} x^2(t-i) - \hat{\mu}_f^2 \quad (4)$$

$$\sigma_s^2(t) = \frac{1}{T_s} \sum_{i=0}^{T_s-1} x^2(t-i) - \hat{\mu}_s^2$$

where $\sigma_f(t)$ and $\sigma_s(t)$ correspond¹ to the respective outputs of the ‘fast’ and ‘slow’ volatility filters, such that, $T_f < T_s$ and $\hat{\mu}_f, \hat{\mu}_s$ correspond to the sample mean of the respective ‘fast’ and ‘slow’ window sizes. The proposed estimate of the instantaneous volatility $\sigma_o(t)$ is a convex combination of the above filters, that is,

$$\sigma_o(t) = \lambda(t)\sigma_f(t) + (1 - \lambda(t))\sigma_s(t - T_d) \quad (5)$$

where $\lambda(t)$ is updated adaptively using the collaborative adaptive filter architecture outlined in [14] [15] and T_d is a time delay introduced for the ‘slow’ volatility filter². The squared error, $e^2(t)$, that the collaborative adaptive filter seeks to minimize is defined as the difference between the desired signal, $\sigma_d(t)$, and the estimated volatility, $\sigma_o(t)$, that is,

$$e^2(t) = (\sigma_d(t) - \sigma_o(t))^2, \quad (6)$$

where $\sigma_d(t)$ is defined as

$$\sigma_d^2(t) = \frac{1}{T_d} \sum_{i=-N_a}^{N_b} x^2(t-i) - \hat{\mu}_d. \quad (7)$$

furthermore, $\hat{\mu}_d$ corresponds to the sample mean. The desired

¹We now refer to the volatility filters with relatively small and large window sizes as ‘fast’ and ‘slow’ filters respectively, this is to reflect the convergence speed of the filters when transient changes in the signal volatility occurs.

²By introducing the time delay, for transient changes in the variance the squared error between $\sigma_o(t)$ and $\sigma_d(t)$ is larger for more time samples thereby increasing the likelihood for the filter to converge onto the ‘fast’ filter given a change in the variance.

Algorithm 1: Adaptive Filtering Based Change Detection

Require:

- Input signal $x(t)$
- Select: $\mu, T_s, T_f, T_d, N_a, N_b, \gamma$.
- Set: $\lambda(1) \leftarrow 1, t \leftarrow 1, \rho \leftarrow 0.001, T_r = 1.2T_s$.

while $t < N$ do

- $\sigma_o(t) \leftarrow \lambda(t)\sigma_f(t) + (1 - \lambda(t))\sigma_s(t - T_d)$.
- $e(t) \leftarrow \sigma_d(t) - \sigma_o(t)$.
- $\lambda(t+1) \leftarrow \lambda(t) + \mu(|\lambda(t)| - \rho)e(t)(\sigma_f(t) - \sigma_s(t - T_d))$

if $\lambda(t+1) \geq \gamma$ and $\text{Flag}(t) = 0$ then

- $s(t) = 1$ in the interval $[t, t + T_r]$.
- $\mu \leftarrow \frac{\mu}{\text{Var}(x(t))}$ in the interval $[t, t + T_r]$.
- $\text{Flag}(t) = 1$ in the interval $[t, t + T_r]$.

end if

- $t \leftarrow t + 1$

end while

signal $\sigma_d(t)$ provides a coarse estimate of the instantaneous volatility so as to enable the collaborative adaptive filter to track changes in volatility³; to this end, a typical window length of $|N_a - N_b| \approx 10$ is recommended. It should be noted that the proposed method converges onto the ‘slow’ volatility filter under steady state conditions, however, large variations in the weight estimate, $\lambda(t)$, were found when performing simulations. To this end, we propose to use the signed sparse-least mean squares (SS-LMS) algorithm [18], that is the minimised cost function which contains both the quadratic error along with a constraint that reduces variation of, $\lambda(t)$, as it converges to ‘slow’ volatility filter. Accordingly, the update of, $\lambda(t)$, is given by⁴

$$\lambda(t+1) = \lambda(t) + \mu(|\lambda(t)| - \rho u)e(t)(\sigma_f(t) - \sigma_s(t - T_d)) \quad (8)$$

where μ is the learning rate of the adaptive filter, ϵ is a positive constant for regularization, ρ is a parameter selected so as to reduce the variability of, $\lambda(t)$ and u corresponds to a Gaussian distributed random variable (please see Appendix B for a more detailed explanation). The estimated convex weight parameter is then mapped to the output of the binary state change sequence $s(t)$, that is, $s(t) = \begin{cases} 1, & \lambda(t) \geq \gamma \\ 0, & \lambda(t) < \gamma \end{cases}$, where $s(t) = 1$ corresponds to a change in the volatility of the time series, while $s(t) = 0$ corresponds to no change. Algorithm 1 summarizes the proposed method referred to as the adaptive filtering based change detection (AFCD). It should be noted that after a change has been detected, normalisation of the learning rate is carried out so as to ensure that the proposed method is independent of the signal scale. Finally, it should be noted that the proposed method assumes that the time index differences between change point locations are greater than T_r samples, owing to the time period required for the estimation

³Note that future samples are also used for estimating the desired signal, as the adaptive filter follows the changes in volatility that is measured by the desired signal.

⁴A hard threshold is applied so that $0 \leq \lambda(t) \leq 1$, that is,

$$\lambda(t) = \begin{cases} 1, & \lambda(t) \geq 1 \\ 0, & \lambda(t) \leq 0 \end{cases}$$

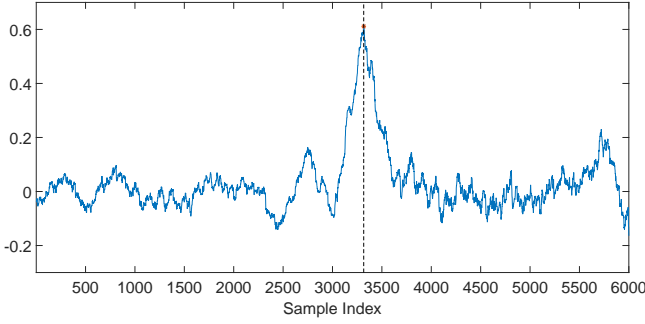


Fig. 3. The output of the volatility filter (of window size T) (dashed line).

of the variance as well as the convergence of the filter to the ‘slow’ volatility filter after a change has been detected.

Remark. *The adaptive filtering based change detection algorithm requires nine input parameters. However, for most problems (verified experimentally) the parameters $\rho = 0.001$, $T_r = 1.2T_s$ and $T_d \approx 300$ are fixed. While, depending on the characteristics of the signal fine tuning of the window sizes T_s, T_f, N_a, N_b and the learning rate μ may be required.*

Algorithm 2 proposes a cooperative change detection algorithm via an extension of the adaptive filtering based change detection algorithm. That is given a multichannel signal we seek to propose a cooperative strategy between the sensors for improved detection of transition points in volatile and dynamic time series data. This is achieved by utilising the combine then adapt (CTA) strategy of the diffusion LMS which is proposed in [16]. Where given N sensors such that each sensor i has an input signal $\mathbf{x}_i(t)$, desired signal $d_i(t)$ and parameters $\mathbf{w}_i(t)$, where each sensor also has the ability to send and receive state estimates to one another⁵, accordingly the CTA strategy for cooperative adaptive filtering is given by [16]

$$\begin{aligned} \boldsymbol{\psi}_i(t) &= \sum_{l \in \mathcal{N}_i} c_{il} \mathbf{w}_l(t-1) \\ \mathbf{w}_i(t) &= \boldsymbol{\psi}_i(t) + \mu_i (d_i - \boldsymbol{\psi}_i^T(t) \mathbf{x}_i(t)) \mathbf{x}_i(t) \end{aligned} \quad (9)$$

The update of the LMS is carried out with respect to the averaged estimates of the LMS output from the previous time instants, where \mathcal{N}_i corresponds to the set of sensors connected to the i^{th} sensor and c_{il} corresponds to the combiner of the sensor estimates. Algorithm 2 provides an overview of the cooperative adaptive filter based change detection (CAFCD) algorithm for multi-sensor data.

B. Parameter Selection

In this section we will explain the rationale behind the selection of parameters for our proposed AFCD and CAFCD algorithms. In particular, consider the following example: a sequence of Gaussian distributed data points with unit variance between sample indices $1 \leq t < 200$ and variance 4 between $200 \leq t \leq 500$. During the transition sample index, it can

⁵The diffusion LMS algorithm considers sensor networks, that is, all the sensors are not fully connected. However, in this work we consider devices where the same information is being recorded and thus we use full cooperation between all the sensors.

Algorithm 2: Cooperative Adaptive Filtering Based Change Detection

Require:

- Input signal $x_c(t)$
- Select: $\mu_c, T_{s,c}, T_{f,c}, T_{d,c}, N_{a,c}, N_{b,c}, \gamma_c$.
- Set: $\lambda_c(1) \leftarrow 1, t \leftarrow 1, \rho_c \leftarrow 0.001, T_{r,c} = 1.2T_{s,c}$.
- $\boldsymbol{\psi}(1) \leftarrow \sum_{c=1}^{N_c} \lambda_c(1)$
- while** $t < N$ **do**
- for** $c = \{1, \dots, N_c\}$ **do**
- $\sigma_{o,c}(t) \leftarrow \boldsymbol{\psi}(t) \sigma_{f,c}(t) + (1 - \boldsymbol{\psi}_s(t)) \sigma_{s,c}(t - T_{d,c})$.
- $e_c(t) \leftarrow \sigma_{d,c}(t) - \sigma_{o,c}(t)$.
- $\lambda_c(t+1) \leftarrow \boldsymbol{\psi}_c(t) + \mu_c (|\boldsymbol{\psi}(t)| - \rho_c) e_c(t) (\sigma_{f,c}(t) - \sigma_{s,c}(t - T_{d,c}))$
- end for**
- $\boldsymbol{\psi}(t+1) \leftarrow \sum_{c=1}^{N_c} \lambda_c(t+1)$
- if** $\boldsymbol{\psi}(t+1) \geq \gamma_c$ and $\text{Flag}(t) = 0$ **then**
- $s(t) \leftarrow 1$ in the interval $[t, t + T_r]$.
- $\mu_c \leftarrow \frac{\mu_c}{\text{Var}(x_c(t))}$ for $[t, t + T_r]$.
- $\text{Flag}(t) = 1$ in the interval $[t, t + T_r]$.
- end if**
- $t \leftarrow t + 1$
- end while**

be observed that the desired signal has risen to the new estimate of the variance, while it can be observed that the ‘fast’ volatility filter has risen before the ‘slow’ volatility filter. Therefore, given a transient change in the volatility, in order to increase the likelihood for the convex parameter $\lambda(t)$ to converge to the ‘fast’ filter, the absolute difference between the ‘fast’ and ‘slow’ volatility filters need to be as large as possible; this implies that the window size for ‘fast’ volatility filter needs to be as small as possible (e.g. 10 sample indices), while the ‘slow’ volatility filter requires a very large window size. This results in a trade off between accuracy (that is the likelihood of detecting a transient change) and the ‘resolution’ (that is the sample difference between two consecutive transient power changes) for both AFCD/CAFCD.

C. Volatility Change Estimator

The volatility change estimator (VCE) seeks to estimate the location of the change points. This is achieved by first obtaining the difference from the output of the volatility filter, $\sigma_x(t)$, with window size, T , as follows

$$\sigma_D(t) = \sigma_x(t) - \sigma_x(t - T), \quad (10)$$

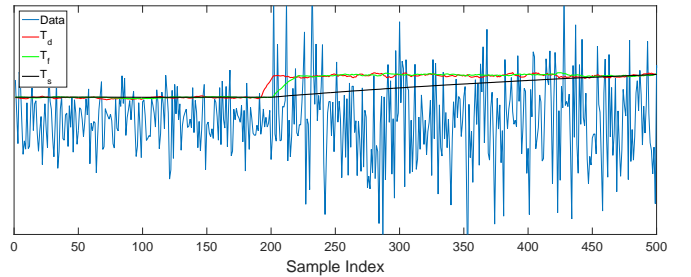


Fig. 4. Data (blue) with change point at sample index 200. The corresponding volatility filters with ‘slow’ window size T_s , ‘fast’ window size T_f and the desired window size T_d .

that is the difference between the output of the volatility filter at the current time index t and at the output of the volatility filter at time index $t - T$. In order to develop a change point location estimator, we first observe the following property in the plot of $\sigma_D(t)$ with respect to sample indices. That is, consider the following example, where a zero mean piecewise stationary (with respect to variance) Gaussian distributed sequence of data points with a change in the variance at the time index 3001. The corresponding plot of $\sigma_D(t)$ is shown in Fig. 3). Observe that $\sigma_D(t)$ oscillates (with an approximately constant variation) around the zero until the change point at sample index 3001, where $\sigma_D(t)$ increases significantly (with respect to the prior variation in $\sigma_D(t)$) and at approximately $3000 + T$ samples the time series hits a maximum (shown by the dashed line in Fig. 3), as a result the following estimator is proposed as a change point location estimate

$$\hat{\tau}_k = \arg \max_t |\sigma_d(t)| - T + 1. \quad (11)$$

While the proposed change point location estimate is an unbiased estimate for a single power change in the time series data (shown in Appendix C), a set of rules are required to deal with multiple change point locations. If a change has been detected by the AFCD algorithm, the estimator in (11) is applied in the interval between the change point detection time to $2T$ samples after the detection.

IV. SIMULATIONS

The proposed methods were verified on both synthetic and real world data, where in particular a comprehensive comparison in the performance is carried out with the generalised likelihood ratio test method and the sequential MDL algorithm. It should be noted that we have not carried out a comparison with the K-SVM method because of its computational complexity.

A. Synthetic Signal

The first synthetic simulation consists of the univariate time series, $x(n)$, consisting of data points drawn from a Gaussian distribution with instantaneous changes in the variance at random points in time. The instantaneous power changes for each segment were selected randomly along with the number of samples in the segment as well as the total signal length. The total number of samples was selected uniformly between $[10000, 40000]$ and each segment length was selected with uniform probability between the interval $[1000, 4000]$. Furthermore, the variance for each segment was dependant on the variance of the prior segment; that is, a scale increase or decrease was selected with equal probability. The magnitude of the scale decrease was selected with uniform probability between $[0.1, 0.7]$ and similarly for a scale increase $[1.5, 4.5]$.

In order to quantitatively evaluate the performance of the respective algorithms, we utilised the following measures: the number of false positives (calculated with respect to each time instant) and false negatives (calculated with respect to the event), the detection latency (the time between the event occurring and the corresponding first detection) and the absolute

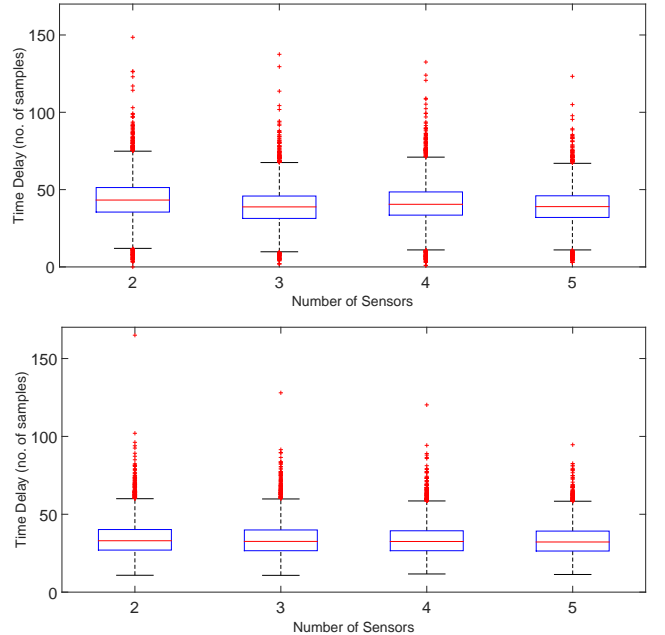


Fig. 5. Figures showing the box plots of the detection latency delays for both the CGLR method (upper panel) and the proposed CAFCD method (lower panel).

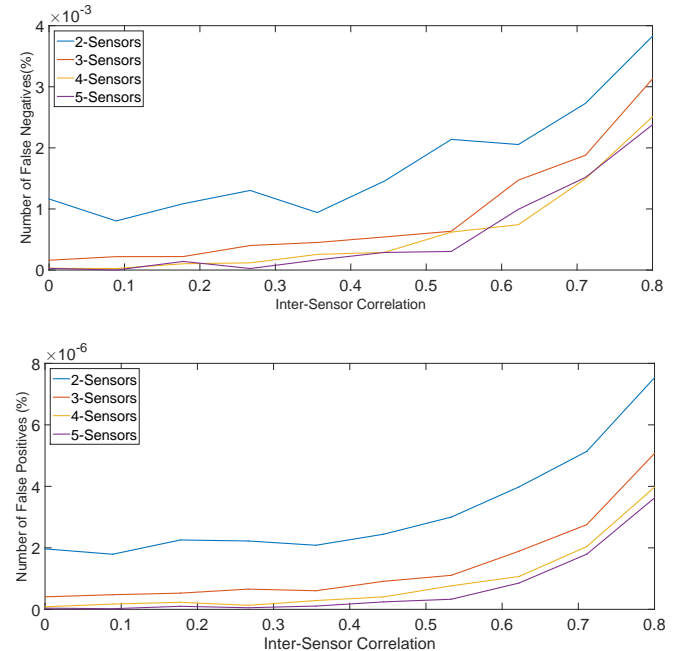


Fig. 6. Number of false negatives (upper panel) and number of false positives (lower panel) for the CAFCD as both the correlation between the sensors is varied and the number of channels.

error in the change point location estimate⁶. The following parameters were selected for the respective algorithms: 1) MDL: window size 150, 2) GLR: window size 100, threshold 8, 3) AFCD: $T_d = 250, T_f = 20, T_d = 300, \mu = 0.35, \gamma = 0.8, N_a = 9, N_b = -1$.

Table I shows the results of the respective algorithms on the

⁶Not applicable for the adaptive filtering based change detection algorithm.

TABLE I

UNIVARIATE (SINGLE SENSOR) SIMULATED DATA RESULTS. THE RESULTS WERE ARE AVERAGES OBTAINED FROM SIMULATIONS CONDUCTED ON 5000 INDEPENDENT TRIALS.

| | MDL | GLR | AFCD |
|----------------------------|-----------------------|-----------------------|----------------------|
| Detection Latency | 127.13 | 40.26 | 37.13 |
| Error in Change Point Loc. | 31.42 | 30.34 | 4.09 |
| False Positives (%) | 2.73×10^{-4} | 3.92×10^{-4} | 1.7×10^{-3} |
| False Negatives (%) | 4.11 | 0.071 | 0.60 |

TABLE II

THE FALSE POSITIVE AND NEGATIVES FOR BOTH THE PROPOSED AFCD- X AND CGLR- X ALGORITHMS, WHERE X CORRESPONDS TO THE NUMBER OF SENSORS, AS WELL AS THE TWO DIFFERENT INTER-SENSOR CORRELATIONS OF 0 AND 0.5.

| | CAFCD-2 | CGLR-2 | CAFCD-3 | CGLR-3 | CAFCD-4 | CGLR-4 | CAFCD-5 | CGLR-5 |
|-----------------------|-----------------------|-----------------------|-----------------------|-----------------------|-----------------------|-----------------------|-----------------------|-----------------------|
| False Positives - 0 | 1.64×10^{-4} | 1×10^{-5} | 4.83×10^{-5} | 2.1×10^{-5} | 1.51×10^{-5} | 4.56×10^{-6} | 4.87×10^{-6} | 8.37×10^{-6} |
| False Negatives - 0 | 0.073 | 0.11 | 0.023 | 0.05 | 0.012 | 0.016 | 0.0043 | 0.011 |
| False Positives - 0.5 | 2.83×10^{-4} | 3.24×10^{-5} | 1×10^{-4} | 9.45×10^{-5} | 4.67×10^{-5} | 2.88×10^{-5} | 3.21×10^{-5} | 3.85×10^{-5} |
| False Negatives - 0.5 | 0.19 | 0.17 | 0.081 | 0.26 | 0.054 | 0.073 | 0.03 | 0.12 |

univariate synthetic data. Where it can be observed that the proposed AFCD outperformed all other methods with respect to the detection latency, while the proposed change point location estimator had the smallest error in the estimation of change point location. The percentage of false positives for the MDL, GLR were approximately equal, while the GLR algorithm outperformed all other methods with respect to the number of false negatives.

The next simulation was aimed at analysing the performance of the proposed collaborative adaptive filtering based change detection algorithm, where we assumed that a fully connected network of sensors were recording the same piecewise constant variation in the volatility. That is for each time instant n , there are N_c sensors, which consists of data points drawn from a Gaussian distribution with fixed inter-sensor correlations and with identical instantaneous volatility changes across sensors (as stated in the previous synthetic simulation). The proposed collaborative adaptive filtering based change detection (CAFCD) algorithm was then compared with a modified GLR algorithm (referred to as the combined GLR (CGLR) algorithm); that is the GLR algorithm was applied separately to each sensor, where the resulting output were combined using the statistical mode operation. The number of sensors used in the comparison were varied between two to five, while two states for the inter-sensor correlations between the sensors were considered: 1) zero correlation and 2) correlation of 0.5 between all of the sensors.

Fig. 5 illustrates the box plots corresponding to detection latencies for both the CAFCD and CGLR algorithms⁷. It can be observed that the proposed method is able to detect changes more rapidly (the average improvement across channels is 23%) than the CGLR algorithm. Furthermore, it should also be noted that the upper quartile of the proposed method is approximately equal to the median detection latency delay of

⁷Fig. 5 presents the box plots of the time delays with zero inter-sensor correlation, as similar performance was observed for sensors with non-zero correlations.

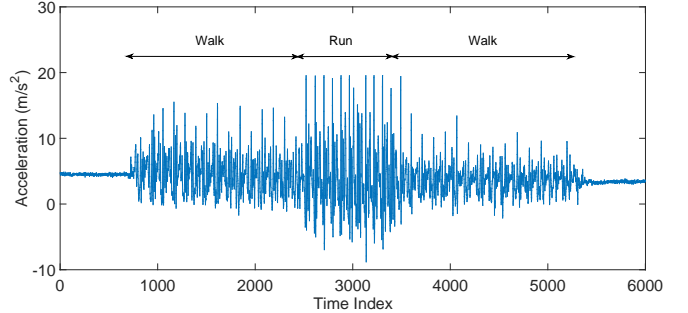


Fig. 7. Figure showing the time domain representation of the accelerometer data, where the three different states of motion in time have been highlighted.

the CGLR method. From Table II it can be observed that the false negatives of the proposed methods were significantly lower than the CGLR for both inter-sensor correlations of 0 and 0.5; however, the false positives for the CGLR were significantly lower than the proposed method for no inter-sensor correlations, while for correlations of 0.5 there was no significant difference between the two methods. This result arises due to the lack of cooperation between the sensors in the CGLR method during the estimation of the state changes; therefore given a set of sensors measuring uncorrelated observations, it is unlikely for a significant number of the sensors to generate false positives within the same time vicinity. Finally, Fig. 6, illustrates the dependence between the false positives and negatives of the proposed CAFCD algorithm as a function of the inter-sensor correlations between all the sensors. Where it can be observed that if the inter-sensor correlations increase above 0.62, the performance of the proposed method degrades with a higher number of false positives and negatives. This increase in false negatives is dependent on the increase in false positives, for example, if a false change has been detected approximately 10 samples before the true change point location. Then the algorithm requires an interval in order to update the normalisation of

TABLE III
THE PERFORMANCE OF THE CAFCD AND CGLR ALGORITHMS ON REAL
WORLD ACCELEROMETER DATA.

| False Negative CAFCD | False Negative CGLR | Proportion CAFCD<CGLR | Latency (No. of Samples) |
|-------------------------|------------------------|--------------------------|-----------------------------|
| 6.52% | 18.48% | 0.64 | 14.78 |

the learning rate, such that during this interval no change can be detected, thus a false negative would arise that is dependent on the false positives (that is a higher number of false positives increases the number of false negatives). In order to overcome this problem for highly correlated time series data, the learning rate of the proposed method needs to be modified.

B. Accelerometer Data

We now analyse the performance of the proposed algorithms on real world tri-axial accelerometer data obtained from a smart phone attached to test subjects (where the data was obtained from [19] that consisted of 23 experimental trials with sampling frequency of 128 Hz). Each experimental trial consists of five different states of motion: ‘no motion’, ‘walking’, ‘running’, ‘walking’ and ‘no motion’; where an example from the output of the accelerometer is shown in Fig. 7. First differencing of the data was also carried out in order to remove trend components in the data (that is, the change in the variance of the residual is carried out). We first compared the proposed collaborative adaptive filtering change detection method with the combined generalised likelihood ratio method. While the underlying true change point locations are unknown, the four different changes in the power of the accelerometer data can be observed via visual inspection (see Fig. 7). As a result, we can obtain the following quantitative performance measures: number of false negatives, the proportion of the CAFCD algorithm detecting the change in variance before CGLR and the relative difference between the detection latencies of CGLR and CAFCD (that is a positive number would indicate CAFCD of having a smaller detection latency from the true change point location). From Table III, it can be observed that the proposed change detection method had a lower number of false negatives when compared with the CGLR algorithm. Furthermore, the proposed method was able to detect more rapidly the transitions in 64% percent of the changes in the states of motion (with approximately 14 samples on average more rapidly).

V. CONCLUSION

This work developed a class of sequential volatility filtering based change detection algorithms, for time series data with instantaneous changes in the volatility. Where the first set of techniques include both the single and multi-sensor adaptive filtering based change detection algorithms, that seek to only detect a change; furthermore, this works also proposes a novel change point location estimator. The proposed algorithms provide a unique way of detecting activities in time series and multi-sensor data. This in particular is very useful in the real world applications and Internet of Things applications

for monitoring and health care domains in which separating and identifying activities from the data is important. Furthermore, the proposed algorithms were compared with existing sequential change detection methods, where a comprehensive performance evaluation was carried out. In particular it was shown that the proposed change detector and location estimator provided an accurate estimation of the change point location, while the proposed single and multi-sensor adaptive filtering based change detection algorithms were able to detect changes more rapidly.

Future work will focus on developing both batch and sequential Monte Carlo Markov Chain based extensions of the proposed volatility filtering algorithms.

VI. ACKNOWLEDGEMENTS

The research leading to these results has received funding from the European Commissions in the H2020 for FIESTA-IoT project under grant agreement no. CNECT-ICT-643943.

APPENDIX A

In order for the collaborative adaptive filter to converge in the steady state onto the ‘slow’ volatility filter, the following condition must hold

$$E\{(\sigma_s(t) - \sigma_d(t))^2\} < E\{(\sigma_f(t) - \sigma_d(t))^2\} \quad (12)$$

that is the mean squared error (MSE) between the output of the ‘slow’ volatility filter with respect to the desired signal must be lower than the MSE between the output of the ‘fast’ volatility filter and the desired signal.

Without loss of generality consider a stationary signal that is normally distributed, $x(t) \sim N(0, 1)$. The corresponding mean squared errors, shown in (12) are given by the following

$$E\{(\sigma_v(t) - \sigma_d(t))^2\} = V\{\sigma_v(t) - \sigma_d(t)\} + (\hat{\sigma}_v(t) - \hat{\sigma}_d(t))^2 \quad (13)$$

where the index v corresponds to the respective ‘slow’ and ‘fast’ volatility filter (shown in (4)), $\sigma_s(t)$ is the desired instantaneous volatility (shown in(7)), $V\{\cdot\}$ is the variance operator and $\hat{\sigma}_v(t)$, $\hat{\sigma}_d(t)$ correspond to the mean of the random variables, $\sigma_v(t) \sim \chi(T_v)$ and $\sigma_d(t) \sim \chi(T_d)$, that form a chi distribution with the following degrees of freedom, T_v and $T_d = |N_a - N_b|$, respectively. It should be noted that the MSE in (13) is equivalent to the sum of the variance and the squared mean of the random variables, $\sigma_v(t)$ and $\sigma_d(t)$. Furthermore, by assuming that $\sigma_v(t)$ and $\sigma_d(t)$ are uncorrelated (this assumption requires that the window sizes, $T_v \gg T_d$), (13) can be written as follows

$$\begin{aligned} E\{(\sigma_v(t) - \sigma_d(t))^2\} &\approx V\{\sigma_v(t)\} + V\{\sigma_d(t)\} + (\hat{\sigma}_v(t) - \hat{\sigma}_d(t))^2 \\ &= \frac{1}{T_v}(T_v - T_v \hat{\sigma}_v^2(t)) + \frac{1}{T_d}(T_d - T_d \hat{\sigma}_d^2(t)) \\ &\quad + (\hat{\sigma}_v(t) - \hat{\sigma}_d(t))^2 \\ &= 2(1 - \hat{\sigma}_d(t)\hat{\sigma}_v(t)) \end{aligned} \quad (14)$$

where

$$\hat{\sigma}_i(t) = \frac{\sqrt{2}}{\sqrt{T_i}} \frac{\Gamma((T_i + 1)/2)}{\Gamma(T_i/2)} \quad \text{for } i = v, d$$

and where, $\Gamma(\cdot)$ is the Gamma function. In order to verify that condition (12) is true, it is necessary to show that (from (14)), $\hat{\sigma}_s(t) > \hat{\sigma}_f(t)$, where this can be seen by using the upper bound of the ratio, $\frac{\Gamma((T_i+1)/2)}{\Gamma(T_i/2)} = \frac{\lceil (T_i+1)/2 \rceil!}{\lfloor T_i/2 \rfloor!} \approx T_i$, (where $\lceil \cdot \rceil$ is the factorial operator, $\lceil \cdot \rceil$ and $\lfloor \cdot \rfloor$ correspond respectively to the ceil and floor functions). As a result, from (14) the proposed algorithm would converge onto the ‘slow’ filter under steady state conditions. Furthermore, it should be noted that if there is a change in the power of the underlying signal being analyzed then the MSE for the ‘fast’ filter would initially be lower than that of the ‘slow’ filter.

APPENDIX B

The SS-LMS algorithm (shown in (8)) is a variation of the gradient descent algorithm used by the conventional least mean squares (LMS) algorithm. It is important to note that the gradient descent algorithm finds the direction of steepest descent, where for one dimensional functions, the direction of steepest descent would be determined by the sign of the function (that is, whether to go uphill or downhill along the function). As a result, from (8), it is important to ensure that the term, $|\lambda(t)| - \rho > 0$, remains positive so as to not affect the direction of the gradient descent algorithm, that is, by setting, $\rho \approx 0$.

It should be noted that the variability in $\lambda(t)$ reduces as the proposed SS-LMS algorithm converges onto the ‘slow’ volatility filter, that is, $\lambda(t+1) - \lambda(t) = \mu(|\lambda(t)| - \rho)u(t) \rightarrow 0$, as $\lambda(t) \rightarrow 0$ and $\rho \approx 0$. Finally, the Gaussian distributed random variable u prevents the estimate of the parameter $\lambda(t)$ from entering and remaining in the following state, $\lambda(t) = \rho$.

APPENDIX C

In this section we verify that the proposed change point estimator (11) is an unbiased estimate for the variance change point location. That is given a sequence of zero mean Gaussian random variables, $x_1, \dots, x_{t-1} \in N(0, \sigma_1^2)$ and $x_t, \dots, x_N \in N(0, \sigma_2^2)$, where the change point occurs at the time index t , the following condition for (11) is satisfied

$$t = E \left\{ \arg \max_{\tau} |\sigma_d(\tau)| \right\} - T + 1 \quad (15)$$

where $E\{\cdot\}$ is the statistical expectation operator and T is the volatility filter window size. Where $\arg \max_{\tau} |\sigma_d(\tau)|$ is equivalent to the following statement

$$E\{|\sigma_d(t+T-1)|\} < E\{|\sigma_d(t+i)|\} \quad i \neq T-1 \quad (16)$$

where i is the set of time shifts such that no further transitions in volatility within $T_i \ll N$ samples of t . This condition ensures that the maximum evaluated for $\arg \max_{\tau} |\sigma_d(\tau)|$, is related to a single instantaneous power change. For multiple instantaneous transitions in volatility, it is assumed that the sample indices difference between two such transition time points is greater than $T_i > 2T$. If the following volatility change conditions $\sigma_2 \geq \sigma_1$ hold, then (16) is equivalent to

$$E\{\sigma_d(t+T-1)\} \geq E\{\sigma_d(t+i)\} \quad i \neq T-1 \quad (17)$$

For $\sigma_2 < \sigma_1$,

$$\begin{aligned} E\{\sigma_d(t+T-1)\} &= E\{\sigma_x(t+T-1)\} - E\{\sigma(t-1)\} \\ &= E \left\{ \sqrt{\sum_{i=0}^{T-1} \frac{x_{t+T-1-i}^2}{T}} \right\} - E \left\{ \sqrt{\sum_{i=0}^{T-1} \frac{x_{t-1-i}^2}{T}} \right\} \end{aligned}$$

we next take the first order Taylor expansion

$$E\{\sigma_d(t+T-1)\} \approx E \left\{ \sum_{i=0}^{T-1} \frac{x_{t+T-1-i}^2}{T} \right\}^{\frac{1}{2}} - E \left\{ \sum_{i=0}^{T-1} \frac{x_{t-1-i}^2}{T} \right\}^{\frac{1}{2}} \quad (18)$$

where it should be noted that the sum of squared standard normal distributed variables are from a chi-squared distribution, that is,

$$\begin{aligned} \sum_{i=0}^{T-1} \frac{x_{t+T-1-i}^2}{\sigma_2^2} &\sim \chi^2(T) \\ \sum_{i=0}^{T-1} \frac{x_{t-1-i}^2}{\sigma_1^2} &\sim \chi^2(T) \end{aligned}$$

As a result, $E\{\sigma_d(t+T)\} \approx \sigma_2 - \sigma_1$. The corresponding estimates for $E\{\sigma_d(t+T+j)\}$ and $E\{\sigma_d(t+T-j)\}$ for $j \neq 1$ are given by

$$E\{\sigma_d(t+T+j)\} \approx \sigma_2 - \sqrt{\frac{(T-j+1)\sigma_2^2 + (j-1)\sigma_1^2}{T}}$$

$$E\{\sigma_d(t+T-j)\} \approx \sqrt{\frac{(T-j+1)\sigma_2^2 + (j-1)\sigma_1^2}{T}} - \sigma_1$$

where it can be easily shown that $E\{\sigma_d(t+T-1)\}$ is less than both $E\{\sigma_d(t+T+j)\}$ and $E\{\sigma_d(t+T-j)\}$, thus illustrating that, $\max_{\tau} |\sigma_d(\tau)|$ provides an unbiased estimate of the change point location.

REFERENCES

- [1] L. D. Xu, W. He, and S. Li, “Internet of things in industries: A survey,” *IEEE Transactions on Industrial Informatics*, vol. 10, no. 4, pp. 2233–2243, 2014.
- [2] B. Xu, L. D. Xu, H. Cai, C. Xie, J. Hu, and F. Bu, “Ubiquitous data accessing method in IoT-Based information system for emergency medical services,” *IEEE Transactions on Industrial Informatics*, vol. 10, no. 2, pp. 1578–1586, 2014.
- [3] S. Maleki, C. Bingham, and Y. Zhang, “Development and realization of change point analysis for the detection of emerging faults on industrial systems,” *IEEE Transactions on Industrial Informatics*, vol. 12, no. 3, pp. 1180–1187, 2016.
- [4] M. Basseville and A. Benveniste, “A new statistical approach for the automatic segmentation of continuous speech signals,” *IEEE Transactions on Information Theory*, vol. 29, no. 5, pp. 709–724, 1983.
- [5] E. Sejdic, C. M. Steele, and T. Chau, “Segmentation of dual-axis swallowing accelerometry signals in healthy subjects with analysis of anthropometric effects on duration of swallowing activities,” *IEEE Transactions on Biomedical Engineering*, vol. 56, no. 4, pp. 1090–1097, 2009.
- [6] F. Desobry, M. Davy, and C. Doncarli, “An online kernel change detection algorithm,” *IEEE Transactions on Signal Processing*, vol. 53, no. 8, pp. 2961–2974, 2005.
- [7] R. Andre-Obrecht, “A new statistical approach for the automatic segmentation of continuous speech signals,” *IEEE Transactions on Acoustics, Speech, and Signal Processing*, vol. 36, no. 1, pp. 29–40, 1988.
- [8] C. Inclan and G. C. Tiao, “Use of cumulative sums of squares for retrospective detection of changes of variance,” *Journal of the American Statistical Association*, vol. 89, no. 427, pp. 913–923, 1994.

- [9] Z. Wang and P. Willett, "Two algorithms to segment white Gaussian data with piecewise constant variances," *IEEE Transactions on Signal Processing*, vol. 51, no. 2, pp. 373–385, 2003.
- [10] M. Lavielle, "Optimal segmentation of random processes," *IEEE Transactions on Signal Processing*, vol. 46, no. 5, pp. 1365–1373, 1998.
- [11] M. Lavielle and E. Lebarbier, "An application of MCMC methods to the multiple change-points problem," *Signal Processing*, vol. 81, pp. 39–53, 2001.
- [12] A. Brandt, "Detecting and estimating parameter jumps using ladder algorithms and likelihood ratio tests," *IEEE International Conference on Acoustics, Speech and Signal Processing*, pp. 1017–1020, 1983.
- [13] C. Alexander, *Moving average models for volatility and correlation, and covariance matrices, Handbook of Finance*. Wiley Press, 2008.
- [14] Y. Zhang and J. A. Chambers, "Convex combination of adaptive filters for a variable tap-length LMS algorithm," *IEEE Signal Processing Letters*, vol. 13, no. 10, pp. 373–385, 2006.
- [15] J. Arenas-García, A. Figueiras-Vidal, and A. Sayed, "Mean-square performance of a convex combination of two adaptive filters," *IEEE Transactions on Signal Processing*, vol. 54, no. 3, pp. 1078–1090, 2006.
- [16] C. G. Lopes and A. H. Sayed, "Diffusion least-mean squares over adaptive networks: Formulation and performance analysis," *IEEE Transactions on Signal Processing*, vol. 56, no. 7, pp. 3122–3136, 2008.
- [17] B. Jelfs and D. P. Mandic, "Signal modality characterisation using collaborative adaptive filters," *1st IAPR Workshop on Cognitive Information Process*, 2008.
- [18] R. Martin, W. Sethares, R. Williamson, and J. C. Johnson, "Exploiting sparsity in adaptive filters," *IEEE Transactions on Signal Processing*, vol. 50, no. 8, pp. 1883–1894, 2002.
- [19] A. Brajdic and R. Harle, "Walk detection and step counting on unconstrained smartphones," *ACM International Joint Conference on Pervasive and Ubiquitous Computing*, p. 225234, 2013.